Tables and figures accompanying the authors' responses to reviews of

High resolution monthly precipitation isotope estimates across Australia from machine learning

Georgina Falster et al.

Correspondence to: Georgina M. Falster (georgina.falster@adelaide.edu.au)

This file contains the following materials:

Table A

Figures A-I

Table A: Relationship of monthly precipitation amount measured at precipitation isotope sampling locations with precipitation amount in the same months as inferred from AGCD v2 and ERA5. Including all sites where precipitation amount was reported alongside precipitation stable isotope composition.

Site	Correlation		Regression coefficient		# months
	AGCD v2	ERA5	AGCD v2	ERA5	# шоппь
Adelaide	0.73	0.63	1.28	0.54	399
Alice Springs	0.97	0.85	1.01	0.87	332
Barakula	0.83	0.71	0.81	0.76	13
Big Hill	0.87	0.71	0.72	0.42	35
Braidwood	0.98	0.83	1.04	0.68	16
Brisbane	0.95	0.82	0.85	0.61	709
Cairns	0.37	0.30	2.81	1.74	1027
Cape Grim	0.83	0.74	0.80	0.66	501
Charleville	0.96	0.85	0.87	0.80	126
Chillagoe	0.60	0.57	2.07	1.83	151
Cobar	0.96	0.76	0.82	0.62	119
Darwin	0.45	0.39	0.54	0.47	1149
Esperance	0.75	0.74	0.69	0.67	20
Evatt	0.91	0.81	0.87	1.12	12
Halls Creek	0.96	0.91	1.10	0.96	15
Horsham	0.92	0.56	0.87	0.66	11
Lithgow	0.96	0.83	1.10	0.88	43
Lucas Heights	0.24	0.18	0.65	0.40	889
Macquarie Marshes	0.35	0.26	0.97	0.72	284
Margate	0.97	0.90	0.83	0.57	18
Meekatharra	0.98	0.73	0.90	0.74	119

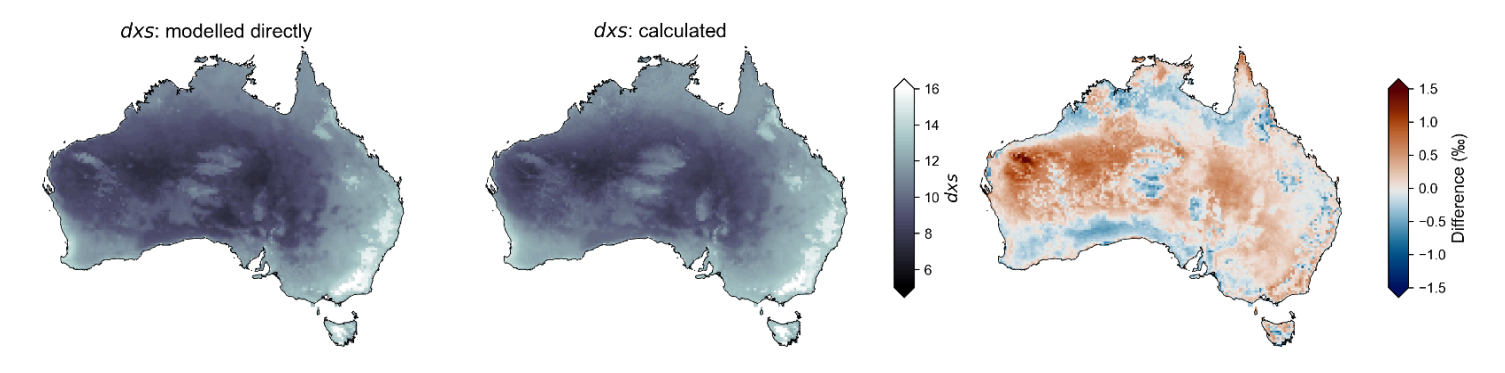


Figure Aa: Maps showing the consequences of modelled dxs_P across the Australian continent directly versus calculating dxs_P from modelled δ^2H and $\delta^{18}O$. First panel shows long-term annual mean precipitation dxs across the Australian continent, modelled directly as described in Section 2.2 (and shown in Fig. 11g). Second panel shows long-term annual mean precipitation dxs across calculated from the random forest-modelled δ^2H_P and $\delta^{18}O_P$ as follows: $dxs_P = \delta^2H_P - 8 * \delta^{18}O_P$. Third panel shows the difference between dxs_P as estimated by the two approaches; the dxs_P values implied by the separate δ^2H_P and $\delta^{18}O_P$ models subtracted from the directly-modelled dxs_P values.

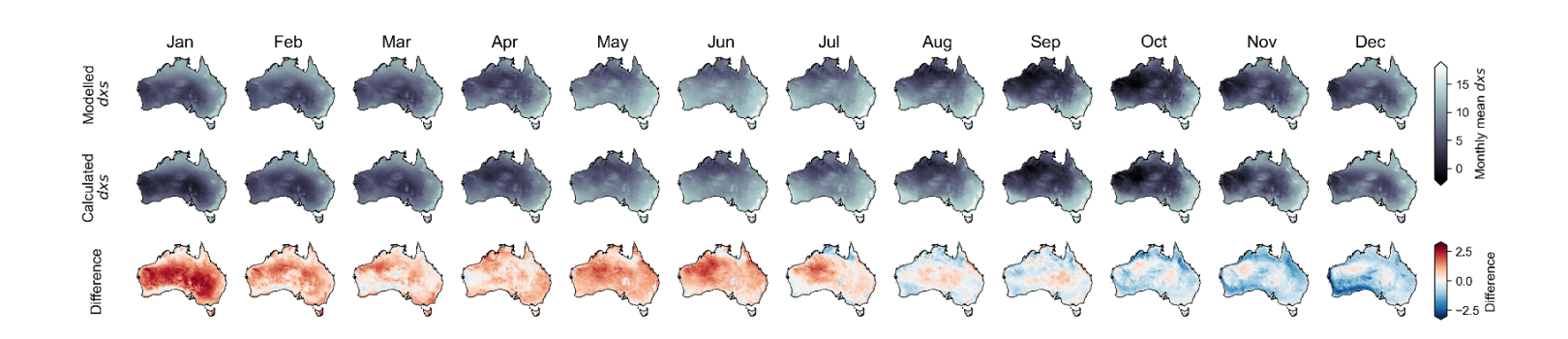


Figure Ab: As per Fig. Aa but showing results for each individual month. Top row shows directly-modelled dxs_P , middle row shows dxs_P as calculated from the random forest-modelled δ^2H_P and $\delta^{18}O_P$, and bottom row shows the difference between the two, calculated as described in Fig. Aa.

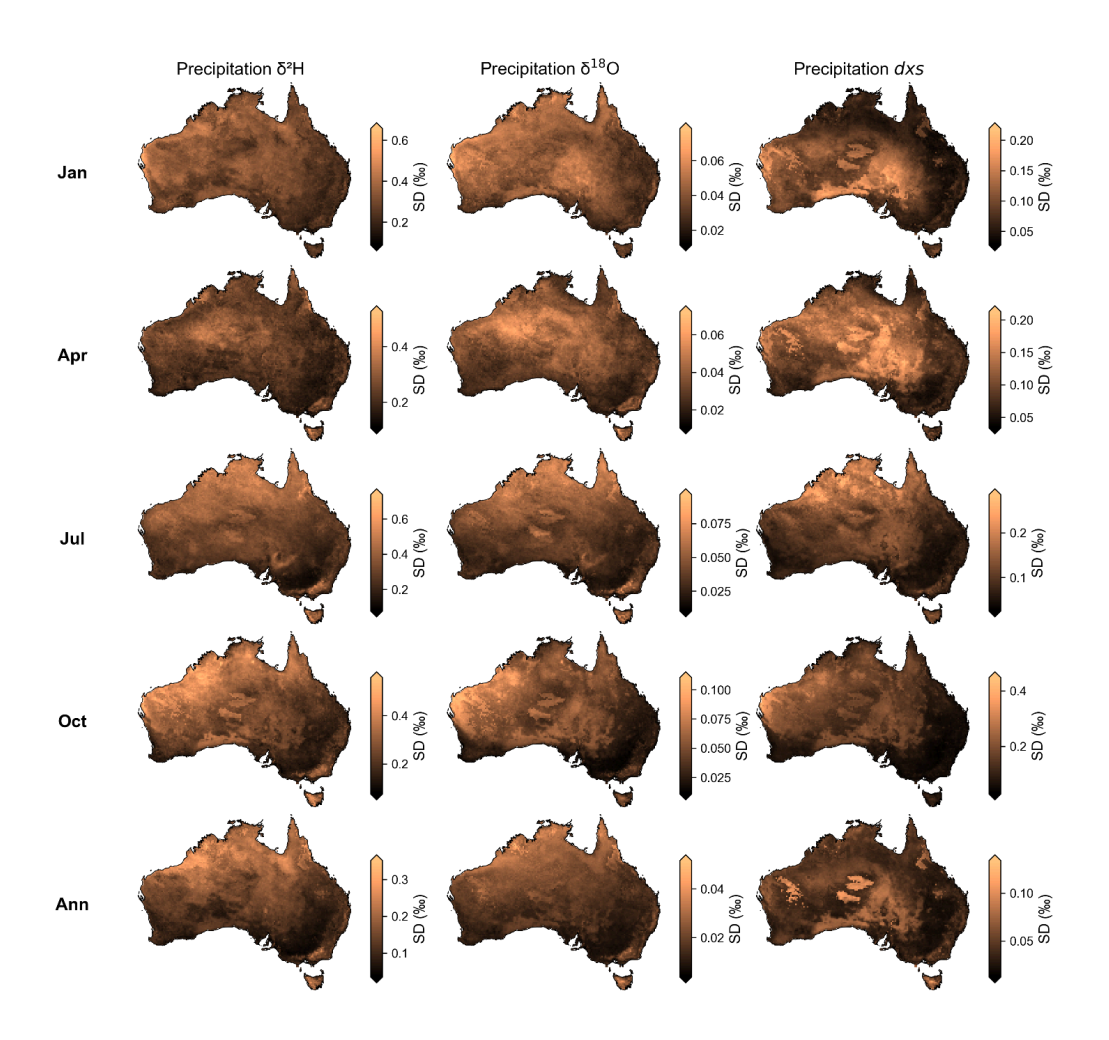


Figure B: Standard deviation of random forest-modelled monthly (rows one to four) and annual (row five) precipitation isotopic variability, across the 50 random forest model ensemble members. Standard deviations calculated on the long-term monthly mean (rows one to four) or precipitation-weighted annual mean (row five), across the 50 models created with unique random seeds. Here showing only the central month of each season. Ensemble standard deviations calculated using the random forest models trained over 1962–2023, using the reduced set of predictor variables (without weather objects).

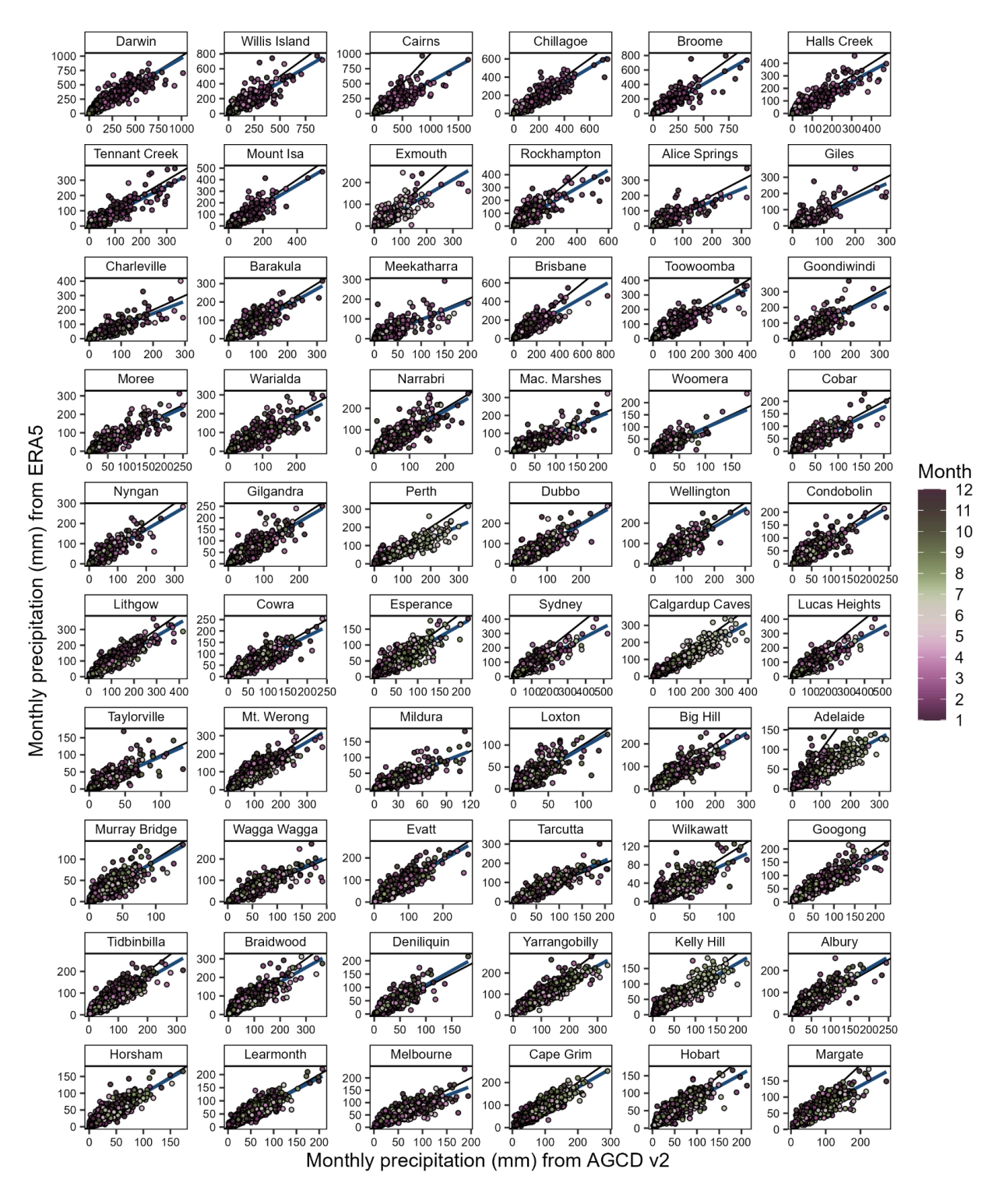


Figure C: Comparison of monthly precipitation amount (1962–2023) estimates from the Australian Gridded Climate Dataset v2 (AGCDv2; Evans et al., 2020) and the European Centre for Medium-Range Weather Forecasts Reanalysis v5 (ERA5; Hersbach et al., 2020). Comparison is shown for each precipitation isotope monitoring sites used in this study; the data were extracted from the grid cell in each product closest to the site. In each panel, the thin black line shows the expected relationship if precipitation in AGCDv2 and ERA5 match exactly (1:1). The blue line shows the linear relationship between AGCDv2 and ERA5 precipitation.

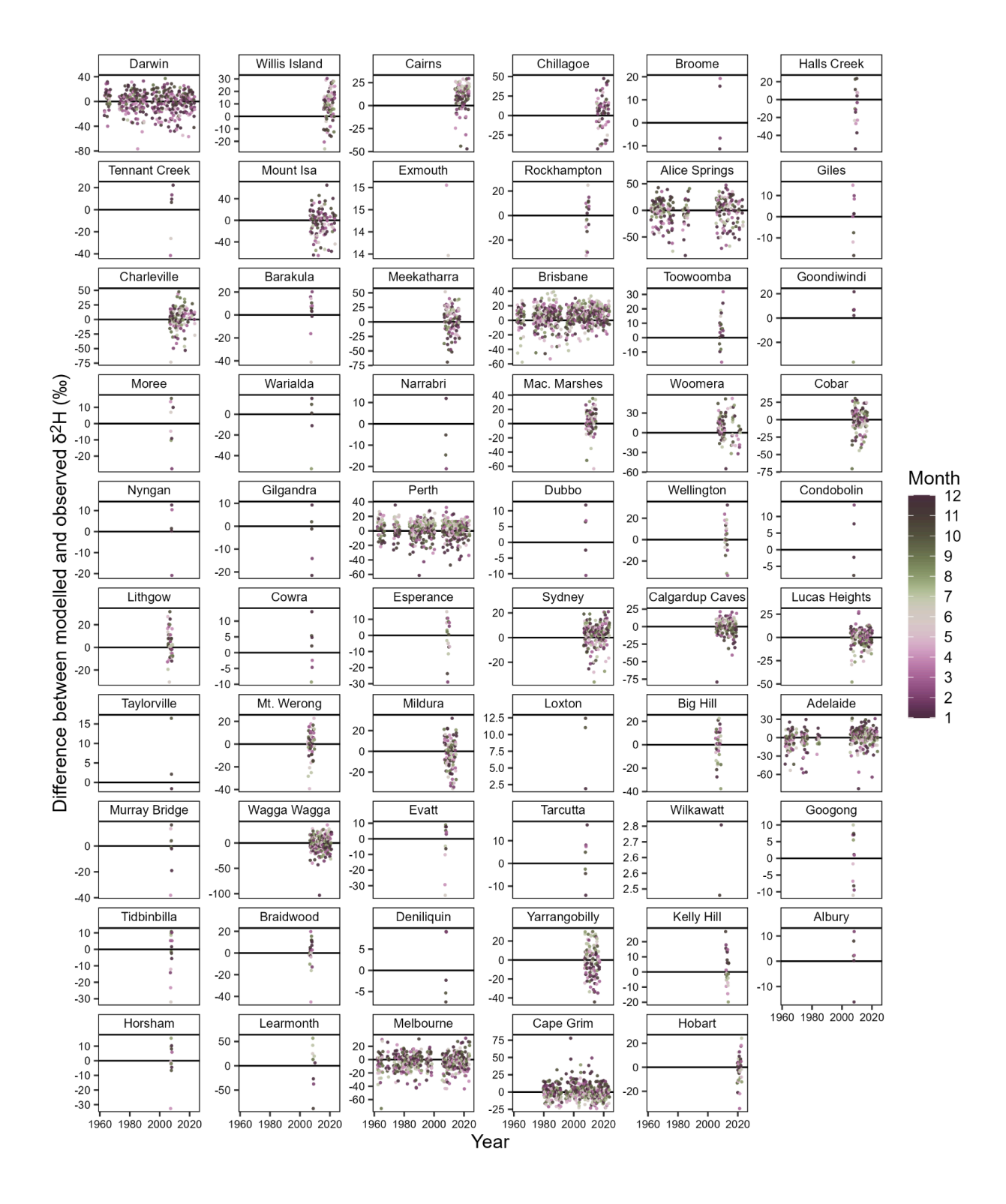


Figure D: Plots showing the difference between modelled and observed monthly $\delta^2 H_P$ values at the 59 sites across Australia with $\delta^2 H_P$ observations. For monthly observation at each site, the observed $\delta^2 H_P$ value was subtracted from the equivalent random forest-modelled $\delta^2 H_P$ value. Sites are arranged by decreasing latitude, with the northern-most site (Darwin) in the top left corner and the southern-most site (Hobart) in the bottom right corner. Site details are as per Table S1. Data points are coloured by month to highlight the seasonal cycle.

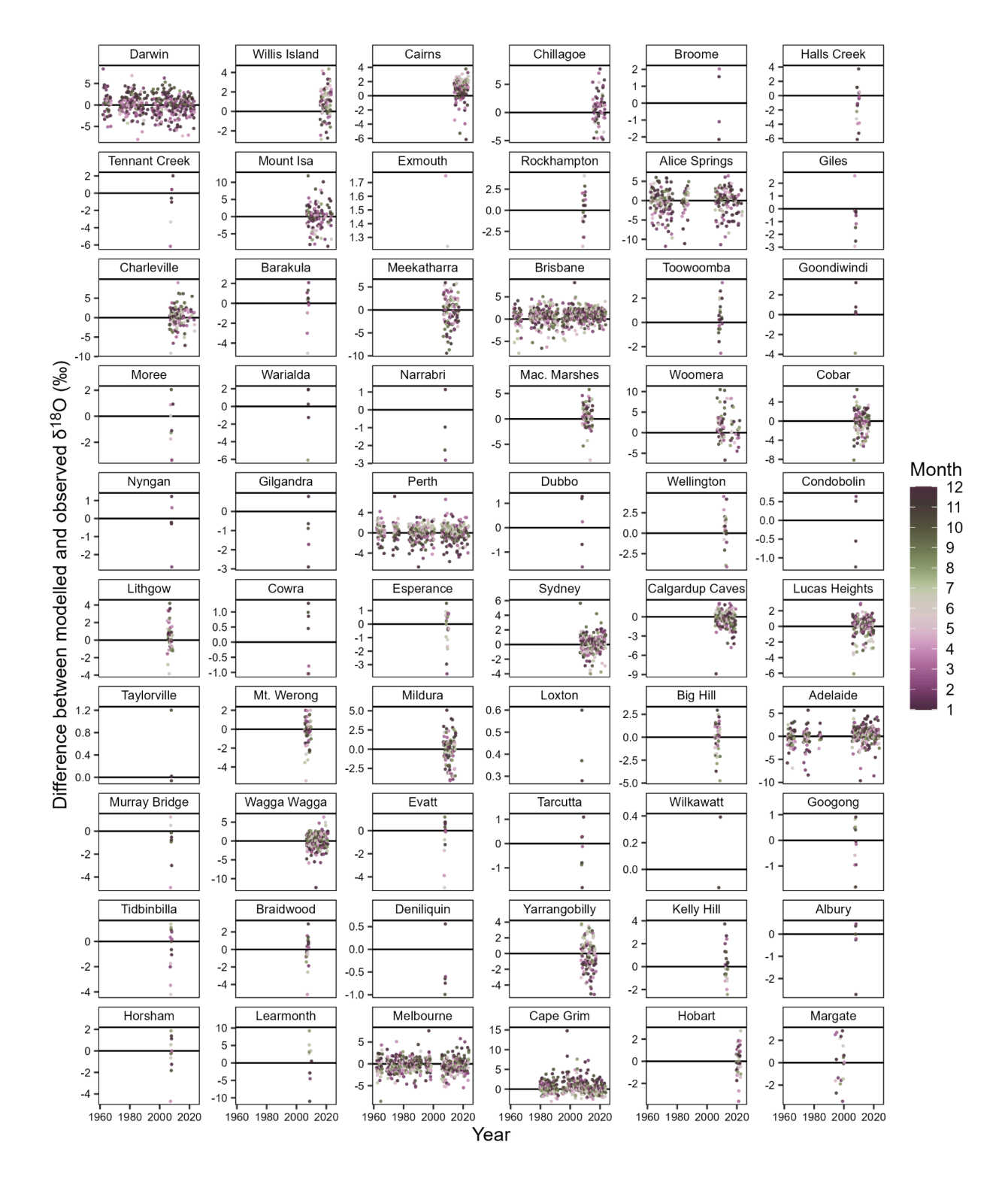


Figure E: As per Figure D but for $\delta^{18}O_P$.

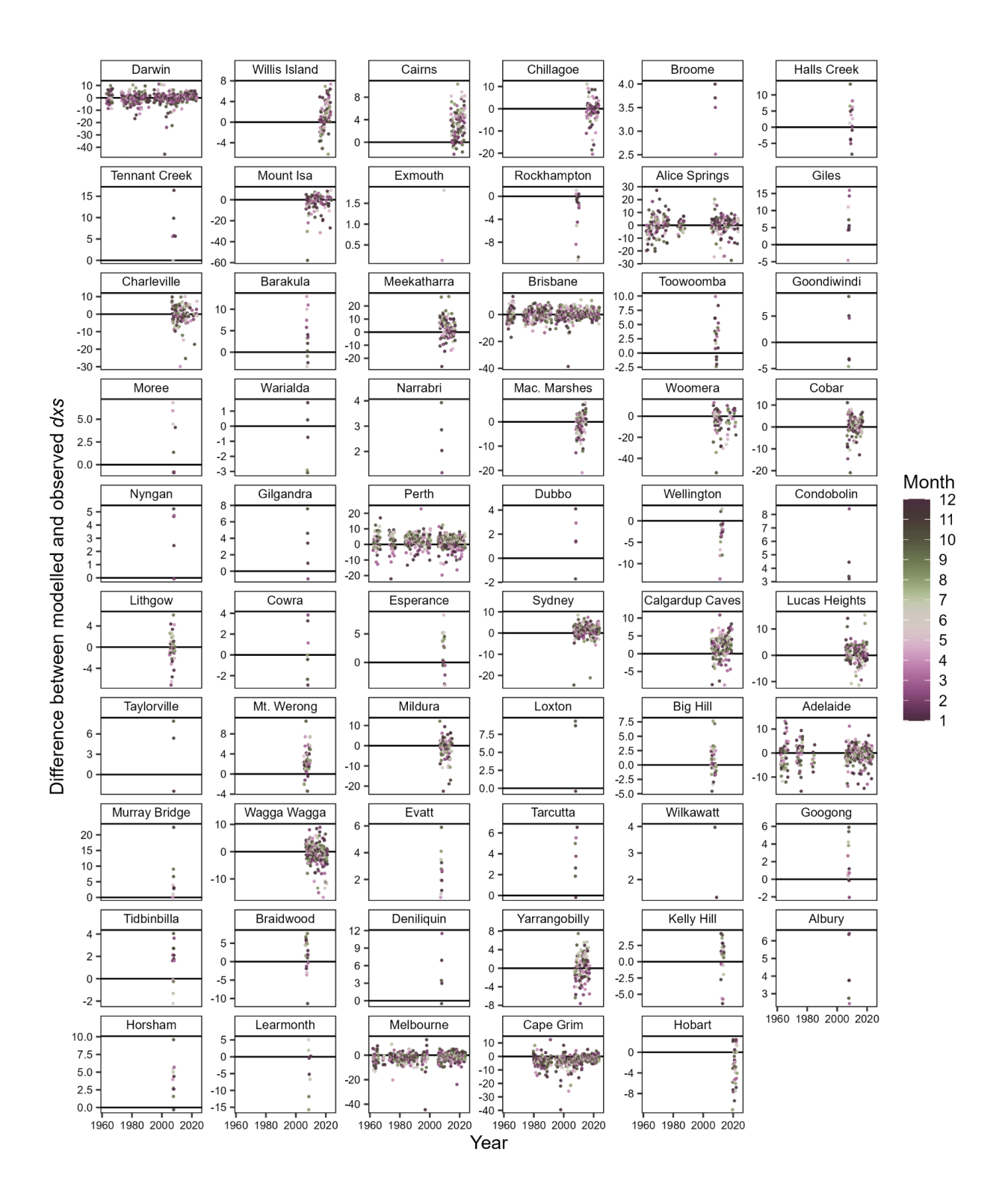


Figure F: As per Figure D but for dxsp.

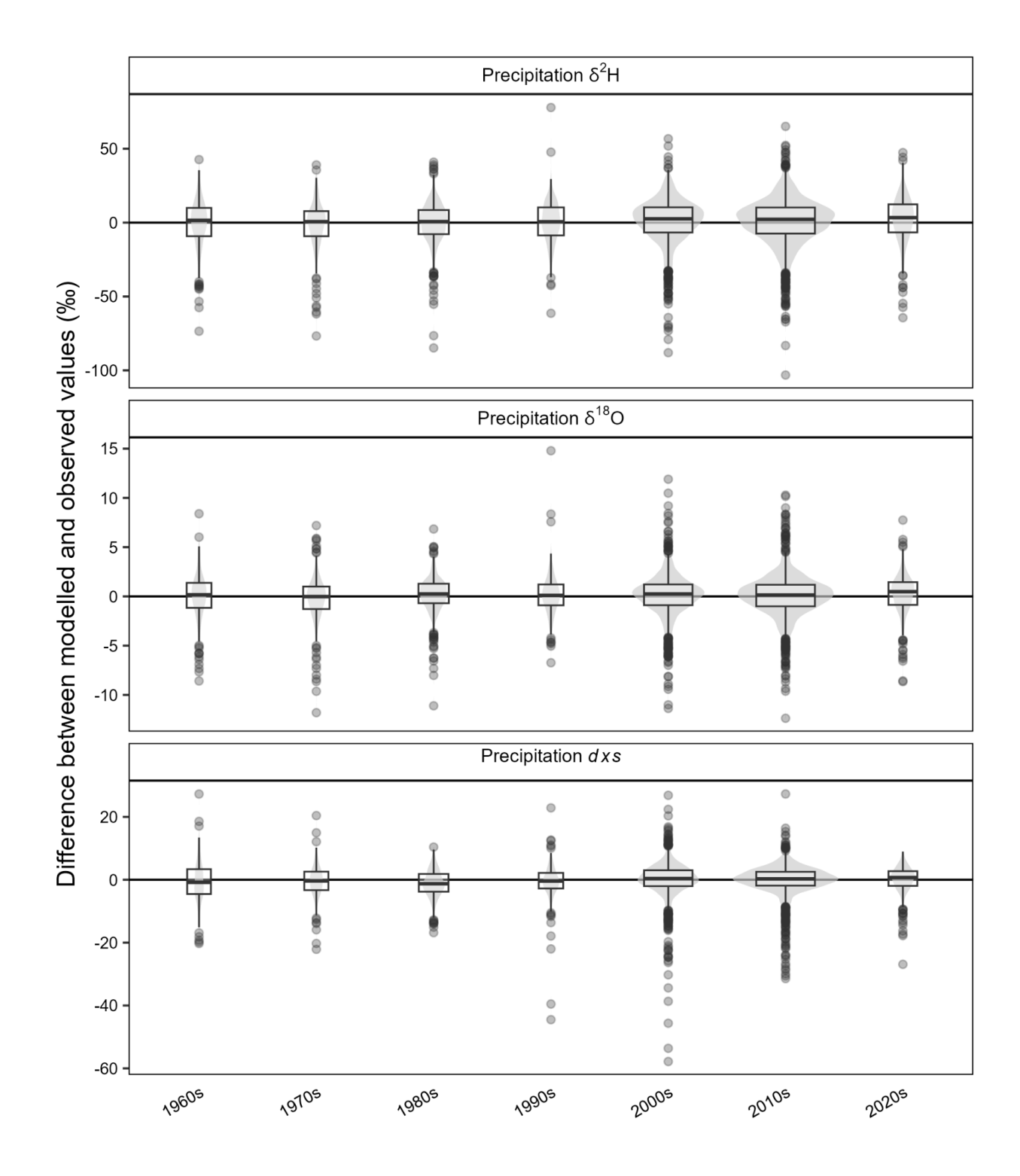


Figure G: Violin-and-boxplots ('voxplots') summarising bias in modelled monthly $\delta^2 H_P$, $\delta^{18}O_P$, and dxs_P values with respect to observed values at the equivalent months/locations. Each distribution summarises all months at all locations for each decade. Modelled values are from the longer models trained over 1962–2023, using the reduced set of predictor variables (without weather objects), and in all cases are the mean of values predicted by 50 unique random forest models, each initiated with a different random seed.

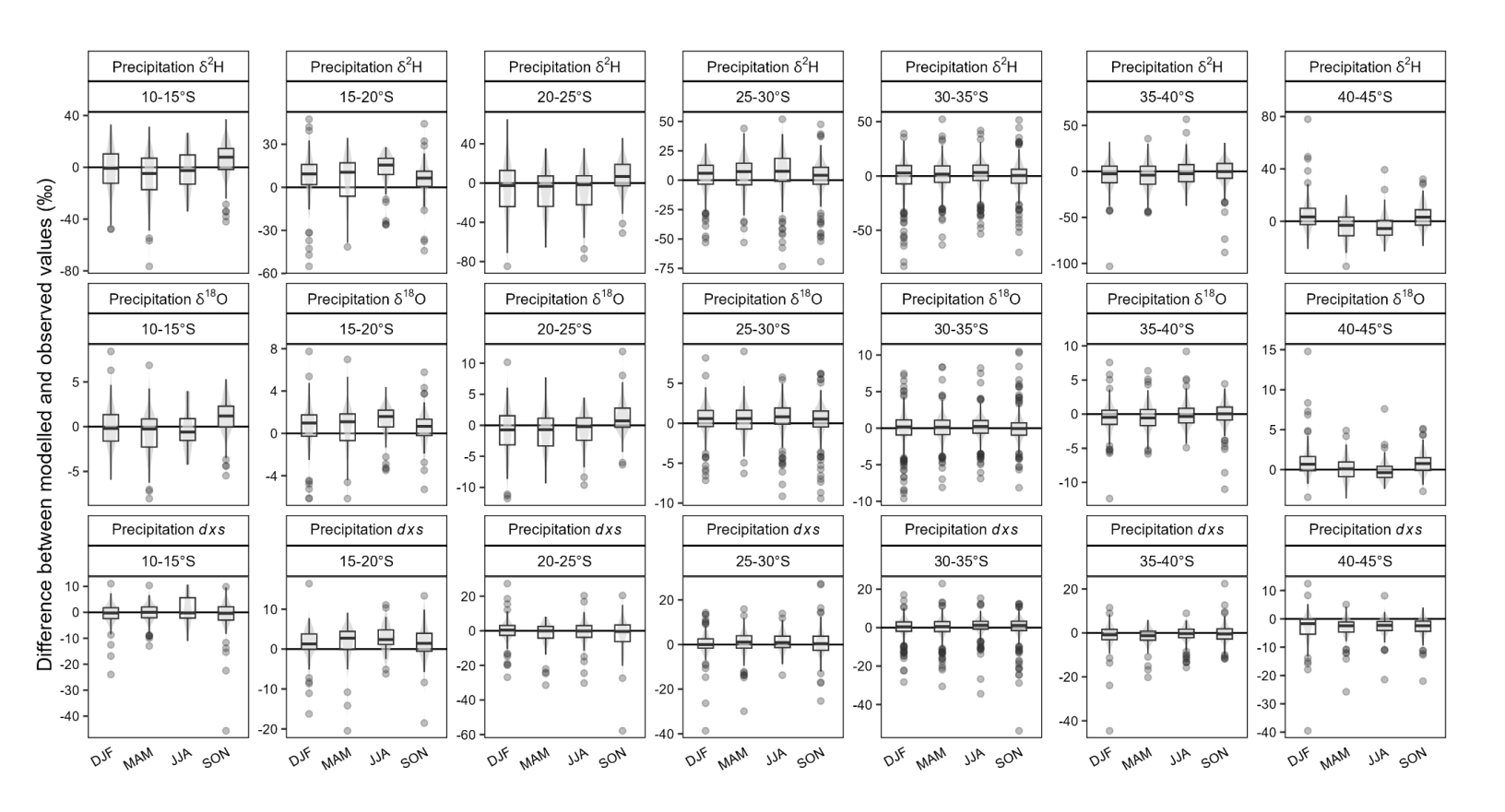


Figure H: As per Fig. G but with bias values summarised by both latitude and season.

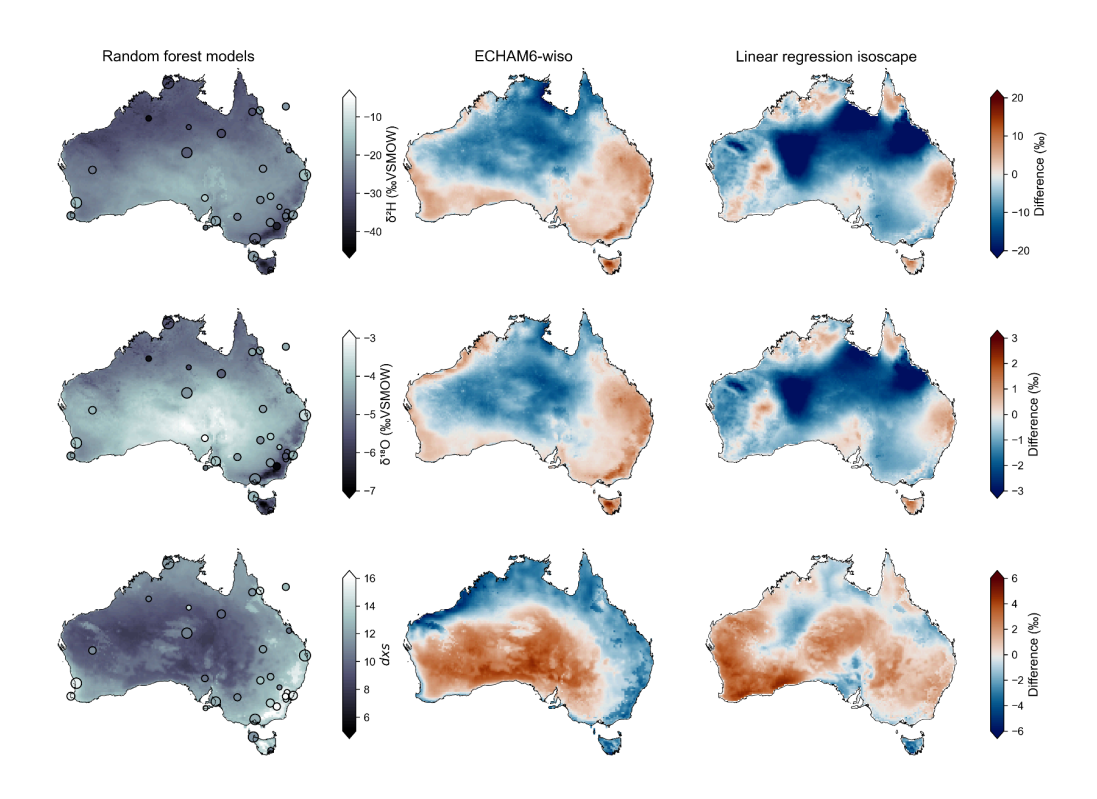


Figure I: Difference in long-term precipitation amount-weighted annual mean precipitation isotopic variability across the Australian continent as estimated by three methods. The first column shows the annual precipitation isotope climatology for $\delta^2 H$, $\delta^{18} O$, and dxs, as calculated from the random forest models described in this paper. The second column shows the difference between the annual precipitation isotope climatology in the random forest estimates and those of ECHAM6-wiso nudged to ERA5 (Cauquoin and Werner, 2021). The third column shows the difference between the annual precipitation isotope climatology in the random forest estimates and those estimated by linear regression using geographical variables (Hollins et al., 2018). Both the ECHAM6-wiso and linear regression isoscapes were regridded to match the spatial resolution of the random forest models using a mass-conservative regridding scheme. After regridding, the ECHAM6-wiso and linear regression estimates were subtracted from the random forest estimate to produce the difference maps shown. Note that the three isoscape climatologies for each metric were calculated using data spanning different time periods (see Fig. 11 caption for details). Points in the first column show the long-term annual mean precipitation isotopic values at each site with 2 or more years of observations (see Section 2.4 for details). Point sizes scale log-linearly with record length (in years).